CHAPTER 3

Electronic and Photophysical Properties of 2-(2′-Hydroxyphenyl) benzoxazole and Its Derivatives Enhancing in the Excited-State Intramolecular Proton Transfer Processes: A TD-DFT Study on Substitution Effect

3.1 Introduction

Due to its intrinsic photophysical property showing a large Stokes shift driven by the excited state intramolecular proton transfer (ESIntraPT), 2-(2′-hydroxyphenyl)-benzoxazole (HBO) comprising the hydroxyl group (O–H acting as a proton donor) and the benzoxazole group (a nitrogen atom acting as a proton acceptor) has become an interesting compound [37, 56, 65-67, 72, 91-93, 120]. Typically, molecules exhibiting ESIntraPT thermodynamically favor enol form (S_0 enol) in the ground state (S_0), which is stabilized by the intramolecular hydrogen bonding, however, upon photoexcitation a fast proton transfer (PT) reaction from the excited enol (S_1 enol) triggers to give the excited keto tautomer (S_1 keto) in subpicosecond time scale [91]. After decaying radiatively to the ground keto form (S_0 keto), the reverse PT takes place to its initial enol form (Figure 2.1). Because of their unique optical property given by the ESIntraPT, HBO and its derivatives have been employed as luminescent material [4, 5], chemical sensors for zinc (II) [121] and anions [122], light-emitting diode devices [3], optical switching [123, 124], and fluorescent probe [6, 7]. In general, fluorescence spectra of these molecules exhibit both enol and keto emission. However, as the ESIntraPT has emerged as one of the most appealing mechanisms for chemosensing applications [5, 9], it is desirable to control their conformers to give only keto emission.

The photophysics of HBO as the parent compound in our present work has been widely studied experimentally [7, 64, 65, 67, 91-93, 97, 98, 125] and theoretically

[102-104, 106, 110, 126-131] because of its structural simplicity and easily chemical modification. Thus, its derivatives [69, 101, 122, 126, 128, 132] have also been increasingly investigated both in experiment and theoretical studies. The photophysical behaviors driven by ESIntraPT of HBO and its derivatives depend not only on solvents but also on their nature and position of various substituents on the phenol fragment as a substituent can influence the hydrogen bonding strength and consequence PT capability [37].

Recently, Ohshima *et al*. [128] reported a comprehensive comparison of electron donating substituents of methoxy (–OCH_3) in 3′-, 4′- and 5′-positions of the phenol moiety. They summarized that in non-polar solvent, the substitution of methoxy on 3′-position gave two emission peaks for the enol (365 nm) and the keto (525 nm) because of the competitive O–H•••O bonding between the methoxy group and the OH group of the phenol moiety. Introducing methoxy on 4′-position, however, only keto emission (480 nm) was observed, indicating a higher efficiency for ESIntraPT. Moreover, Seo *et al*. [69] reported that the emission of HBO derivative having methoxy (–OCH_3) as an electron donor on 4′-position of the phenol moiety in non-polar solvent gave the keto emission peak at about 466 nm (blue-shifted emission relative to HBO). The keto emission of HBO derivative having cyano (–CN) as an electron acceptor at the same position of the phenol moiety also was blue-shifted ~10 nm (compared to HBO at 506 nm in solid state) as reported by Irgibaeva *et al*. [102]. In addition, Seo *et al*. [69] studied on HBO having carboxaldehyde and ethoxycarbonyl group (–CHO (510 nm) and –$COOC_2H_5$ (480 nm)) substituted at this position. The keto emission was redshift compared to HBO due to the contribution of π-conjugated delocalization with benzoxazole ring.

Despite the unique character and potential applications of such compounds, the practically important spectral adjustment of enol absorption and keto emission by different electron donating and withdrawing substituents both on phenol and benzoxazole segments in HBO derivatives has not been fully understood. Moreover, roles of electron donating or withdrawing substituents affecting absorption and emission of its derivatives compared to HBO can be generally elucidated by means of quantum calculations using density functional theory (DFT). Nowadays, DFT and its extension

called time-dependent DFT (TD-DFT) have become reliable standard tools to describe electronic structures and optical properties of chemosensing molecules [5, 98]. It has been known that fluorescent dyes that emit in the red and higher regions of wavelength (low energy) are often more favorable for biological imaging applications because they cause less photodamage during cell imaging [133]. Based on available photophysical properties of some selected molecules of HBO derivatives, only keto emission from those molecules was focused as a reference to validate our method of choice to predict other available molecules, in which their photophysical properties have not been reported before. These selected molecules are representatives of HBO having electron donating and electron withdrawing groups for utilizing electronic and spectral properties of the ESIntraPT process to control their desirable properties (especially red or blue shift emission). HBO with electron withdrawing groups were introduced to increase the Strokes shift after ESIntraPT taking place.

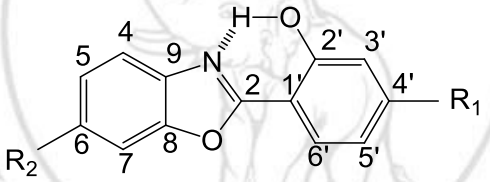

Name	R_1	R_2
HBO	H	H
m-MeHBO	CH_3	H
MHBO	OCH_3	H
CNHBO	CN	H
HBOMe	H	CH_3
HBOM	H	OCH_3
HBOF	H	F
HBOCl	H	Cl
HBOA	H	CHO
HBOE	H	$COOC_2H_5$
m-MeHBON	CH_3	NO_2

Figure 3.1. 2-(2′-Hydroxyphenyl)benzoxazole (HBO) and its derivatives.

To this end, we systematically compared the effect of substitution on spectral characteristics of HBO and its derivatives using theoretical calculations with DFT and TD-DFT. The following substituents placed to two positions: i) 4′-position and ii) 6-position and iii) both 4′- and 6-position of HBO to give ten different HBO derivatives as depicted in Figure 3.1 have been studied:

i) 2-(2′-hydroxy-4′-methylphenyl)benzoxazole (*m*-MeHBO) [126, 134], 2-(2′-hydroxy-4′-methoxyphenyl)benzoxazole (MHBO) [69, 128], 2-(2′-hydroxy-4′-cyano-phenyl)benzoxazole (CNHBO) [102],

ii) 2-(2′-hydroxyphenyl)-6-methylbenzoxazole (HBOMe) [135], 2-(2′-hydroxy-phenyl)-6-methoxybenzoxazole (HBOM), 2-(2′-hydroxy-phenyl)-6-fluoro-benzoxazole (HBOF), 2-(2′-hydroxyphenyl)-6-chlorobenzoxazole (HBOCl) [135], 2-(2′-hydroxyphenyl)-6-cabaldehydeben-zoxazole (HBOA) [69] and 2-(2′-hydroxyphenyl)benzoxazole-6-carboxylic acid ethyl ester (HBOE) [69],

iii) 2-(2′-hydroxy-4′-methylphenyl)-6-nitrobenzoxazole (*m*-MeHBON).

3.2 Computational Details

The geometry optimization of ground state (S_0) equilibrium structures of HBO was performed without symmetry constraints in the gas phase and in solution using five different DFT functionals with various exchange-correlation functional namely B3LYP [81, 82], PBE0 [83], CAM-B3LYP [84], ωB97XD [85], and LC-BLYP [86] with 6-311+G* basis set. The brief details of each functional are as follows: two hybrid B3LYP and PBE0 functionals including 20% and 25% of Hartree-Fock exchange, respectively and three long-range corrected hybrid ωB97XD, CAM-B3LYP, and LC-BLYP functionals, which are Head-Gordon, Handy, and Hirao methods, respectively. Frequency calculations at the same functional and basis set were calculated to confirm that no imaginary frequency was found for the minimum energy structures. To reveal the influence of DFT functional on the absorption spectrum associated with the electronic transition of HBO, the vertical excitation energy and electronic absorption spectra were performed using TD-DFT of all functionals at the same basis set. The effect of solvent such as cyclohexane, which was used in the experiment [97, 125], was taken into account by Self-Consistent Reaction Field (SCRF) method through the non-equilibrium and equilibrium polarizable continuum model calculations using the polarizable conductor calculation model (C-PCM) [136, 137]. The non-equilibrium implementation of the C-PCM framework is LR-PCM, and the equilibrium is SS-PCM, in which the details of both models can be found in Ref. [138]. The validation of all five DFT functionals on describing two main characteristic peaks of *syn*-enol HBO at lower-energy region (longer wavelength) and at higher-energy region (shorter wavelength) attributed to π-π* and n-π* transitions [56, 67], respectively compared to available UV-vis spectrum of HBO. From method of choice, the most suitable one with 6-311+G* basis set for predicting the enol absorption spectra of HBO is B3LYP in the gas phase. This method and basis set were further employed to optimize the S_0 and excited (S_1) states as well as the vertical excitation energy, UV-vis absorption spectra of enol forms, and fluorescence emission spectra of keto forms of HBO derivatives in the gas phase. All calculations were performed using the Gaussian 09 program suit [139].

3.3 Results and Discussion

3.3.1 Effect of DFT Functional

From various DFT functionals, the suitable choice of DFT and TD-DFT is very important to explain the enol absorption characteristics of HBO molecule. Five different functionals (B3LYP, PBE0, CAM-B3LYP, ωB97XD, and LC-BLYP) with 6-311+G* basis set were carried out to obtain S_0 equilibrium structures and to reveal the functional influence on the absorption spectrum in electronic transition using TD-DFT of *syn*-enol HBO, which was confirmed to be the most stable structure compared to its conformers [56, 108, 127] and only *syn*-enol form can give the keto tautomer through the ESIntraPT process [4, 56, 66, 67, 97]. The comparison of various TD-DFT calculations in terms of absorption (nm), oscillator strength (*f*), and deviation between the calculated and experimental wavelength (Δλ) of HBO in the gas phase and in cyclohexane between experimental and computed results was listed in Table 3.1. From the experimental results, absorption peaks of *syn*-enol HBO in the gas phase of an argon matrix at 335 nm (lower energy attributed to π-π*) and at 284 nm (higher energy attributed to n-π*) were reported by Arthen-Engeland *et al*. [91]. The computed results from hybrid functions of TD-B3LYP and TD-PBE0 show slight shift of absorption peaks from the experiment [91] with maximum deviations of 27 nm (π-π*) and 13 nm (n-π*), respectively, which are in good agreement with the experiment. While the long-range corrected functionals (TD-CAM-B3LYP, TD-ωB97XD, and TD-LC-BLYP) provide large differences of both π-π* and n-π* transitions with maximum deviation of 69 and 47 nm for π-π* and n-π*, respectively in which the results from TD-ωB97XD and TD-CAM-B3LYP methods are almost identical.

Table 3.1 Absorption (nm), excitation energy (eV), oscillator strength (*f*), and deviation between the calculated and experiment wavelength (Δλ) of *syn*-enol HBO in the gas phase and in cyclohexane. The calculations were performed using various TD-DFTs at 6-311+G* basis set.

TD-DFT	**Absorption, nm (excitation energy, eV) of π-π***	***f***	**MOs (% contribution)**	**Δλ, nm**	**Absorption, nm (excitation energy, eV) of n-π***	***f***	**Δλ, nm**
Gas phase							
TD-B3LYP	318 (3.90)	0.393	HOMO→LUMO (92%)	-17	280 (4.42)	0.346	-4
TD-PBE0	308 (4.03)	0.423	HOMO→LUMO (93%)	-27	271 (4.58)	0.335	-13
TD-CAM-B3LYP	288 (4.30)	0.463	HOMO→LUMO (89%)	-47	254 (4.88)	0.265	-30
TD-ωB97XD	287 (4.32)	0.461	HOMO→LUMO (87%)	-48	253 (4.90)	0.264	-31
TD-LC-BLYP	266 (4.66)	0.454	HOMO→LUMO (82%)	-69	237 (5.24)	0.202	-47
Experiment [a]	*335* [a] *(3.70)*				*284* [a]		

Cyclohexane (LR-C-PCM)							
TD-B3LYP	322 (3.85)	0.589	HOMO→LUMO (96%)	-12	284 (4.36)	0.345	-1
TD-PBE0	313 (3.97)	0.615	HOMO→LUMO (96%)	-21	274 (4.52)	0.342	-11
TD-CAM-B3LYP	292 (4.25)	0.640	HOMO→LUMO (91%)	-42	257 (4.83)	0.294	-28
TD-ωB97XD	291 (4.26)	0.636	HOMO→LUMO (90%)	-43	256 (4.85)	0.298	-29
TD-LC-BLYP	269 (4.60)	0.608	HOMO→LUMO (84%)	-65	239 (5.19)	0.246	-46
Cyclohexane (SS-C-PCM)							
TD-B3LYP	321 (3.87)	0.340	HOMO→LUMO (93%)	-13	281 (4.41)	0.411	-4
TD-PBE0	310 (4.00)	0.382	HOMO→LUMO (93%)	-24	271 (4.57)	0.384	-14
TD-CAM-B3LYP	288 (4.30)	0.451	HOMO→LUMO (89%)	-46	254 (4.87)	0.279	-31
TD-ωB97XD	287 (4.32)	0.450	HOMO→LUMO (87%)	-47	253 (4.90)	0.278	-32
TD-LC-BLYP	266 (4.66)	0.449	HOMO→LUMO (82%)	-68	237 (5.24)	0.209	-48
Experiment [b]	*334 (3.71)*				*285 (4.23)*		

[a] in an argon matrix [91], [b] in cyclohexane [56] for π-π* and n-π*

In cyclohexane, absorption maxima of HBO at 334 and 285 nm for π-π* and n-π* transitions, respectively were reported by Wang *et al*. [97]. All functionals including solvent effect of cyclohexane (LR-C-PCM) show a slight bathochromic shift (red shift) for both π-π* and n-π* transitions compared with the results in the gas phase. In addition, the oscillator strengths of HBO for all functionals greatly increase about 70% from gas phase to solution indicating the positive enhancement of solvatochromic effect. Absorption maxima computed using hybrid functionals provide a small difference from the experiment. For π-π* (n-π*) transition, the deviations are 12 (1) and 21 (11) nm for TD-B3LYP and TD-PBE0, respectively which are similar to the gas phase results. However, TD-ωB97XD, TD-CAM-B3LYP, and TD-LC-BLYP methods still provide a large deviation from the experiment with values in the range of 42-64 nm (π-π*) and 28-46 nm (n-π*). The oscillator strengths of HBO in cyclohexane from all functionals were found to increase. In addition, solvent effect of cyclohexane (SS-C-PCM) gave a slightly deviation from LR-C-PCM as shown in Table 3.1.

For overall performance of all DFT functionals, long-range-corrected functionals either with small fraction of HF exchange (TD-ωB97XD, TD-LC-BLYP, and TD-CAM-B3LYP) fail to reproduce the experimental results both in the gas phase and in solutions. For normal hybrid function, TD-B3LYP and TD-PBE0 functionals are capable of explaining electronic and spectral properties of HBO, however, the popular TD-B3LYP gives better-computed results compared to available experiment data. Therefore, based on our method validation, TD-B3LYP will be used to further investigate electronic properties of HBO and its derivatives.

Table 3.2 Relative energies (kcal·mol^{-1}) and selected structural parameters (Å and degree) from optimized structures of HBO and its derivatives computed at B3LYP/6-311+G* level (in gas phase).

	State	**HBO**	***m*-Me-HBO**	**MHBO**	**CNHBO**	**HBOMe**	**HBOM**	**HBOF**	**HBOCl**	**HBOA**	**HBOE**	***m*-Me-HBON**
Relative energy	*Enol* S_0	0.00	0.00	0.00	0.00	0.00	0.00	0.00	0.00	0.00	0.00	0.00
	Enol S_1	85.63	85.96	87.06	81.42	85.13	83.29	85.26	84.30	76.98	81.31	79.63
	Keto S_0	10.85	10.50	9.13	9.97	10.71	11.18	11.65	11.57	11.35	11.01	10.55
	Keto S_1	77.80	78.18	79.30	76.08	77.61	78.94	78.03	77.35	65.98	71.60	77.80
O–H	*Enol* S_0	0.983	0.984	0.985	0.984	0.984	0.983	0.982	0.982	0.983	0.983	0.983
	Enol S_1	1.019	1.013	0.999	0.999	1.007	0.992	1.016	1.012	1.036	1.025	0.987
O•••H*	*Keto* S_0	1.732	1.743	1.760	1.747	1.732	1.729	1.722	1.724	1.730	1.726	1.739
	Keto S_1	1.914	1.925	1.973	1.910	1.923	1.921	1.915	1.908	1.916	1.923	1.942
N•••H*	*Enol* S_0	1.825	1.828	1.816	1.821	1.825	1.828	1.834	1.834	1.832	1.828	1.829
	Enol S_1	1.670	1.692	1.749	1.757	1.717	1.788	1.683	1.697	1.612	1.647	1.808

N–H	*Keto* S_0	1.040	1.038	1.036	1.038	1.040	1.040	1.722	1.041	1.040	1.042	1.039
	Keto S_1	1.025	1.024	1.020	1.025	1.024	1.024	1.025	1.026	1.022	1.022	1.023
O•••N	*Enol* S_0	2.685	2.688	2.680	2.680	2.686	2.688	2.691	2.691	2.688	2.686	2.691
	Enol S_1	2.596	2.611	2.647	2.648	2.625	2.671	2.604	2.612	2.555	2.578	2.685
	Keto S_0	2.553	2.559	2.567	2.559	2.553	2.552	2.547	2.652	2.552	2.550	2.558
	Keto S_1	2.655	2.663	2.687	2.646	2.660	2.659	2.656	2.549	2.652	2.658	2.671
NCCC	*Enol* S_0	0.0	0.0	0.0	0.0	0.0	0.0	0	0.0	0.0	0.0	0.1
	Enol S_1	0.0	0.0	0.0	0.0	0.0	0.0	0	0.0	0.0	0.0	0.0
	Keto S_0	0.0	0.0	0.0	0.0	0.0	0.0	0	0.0	0.0	0.0	0.1
	Keto S_1	0.0	0.0	0.0	0.0	-0.2	0.0	0	0.0	0.0	0.0	4.5

* Intramolecular hydrogen bond

3.3.2 Energies and Geometries of HBO and Its Derivatives

HBO and its derivatives (as depicted in Figure 3.1) were optimized with suitable DFT functional at B3LYP/6-311+G* level in the gas phase to study the effect of electron donating and electron withdrawing groups substituted to 4′- and 6-positions to the spectral feature of keto emission. Energies and selected geometry parameters of HBO and its derivatives optimized both in S_0 and S_1 states are summarized in Table 3.2. The energy of *syn*-enol HBO was found to be lowest (most stable) compared to other conformations, which is confirmed by experimental results reported by Abou-Zied [56] and Woolfe *et al*. [67] and our recent work [127]. The energies of enol forms in the ground state are lower (more stable) than those of their keto tautomers about 10 kcal•mol^{-1}. Upon photoexcitation, however, the energies of keto are lower than those of their enol forms especially HBOA and HBOE which are about 11 and 10 kcal•mol^{-1}, respectively as listed in Table 3.2. This lower energy of keto for HBOA and HBOE might be caused by stabilization of electron-withdrawing capability at 6-position of benzoxazole moiety.

From S_1 optimized structures, O–H bond distances of S_1 enol forms of all molecules are in the range of 0.992-1.036 Å, which are longer than their S_0 enol (in the range of 0.982-0.985 Å), corresponding to a decrease of intramolecular hydrogen bond (N•••H) of S_1 enol (stronger hydrogen bond). O–H bond of S_1 enol HBO increases by 0.036 Å compared with its S_0 enol while O–H bond of *m*-MeHBO having a weak electron donor slightly increases by 0.029 Å. However, O–H bonds of *m*-MeHBO, MHBO, and CNHBO are slightly longer about 0.014-0.029 Å than those of their S_0 enol while O–H bond of HBOA and HBOE with a strong electron acceptor is different from its S_0 enol about 0.053 and 0.042 Å, respectively. These substituents make O–H bond of HBO derivatives stronger than that of HBO and the O•••N distances of S_1 enol of all compounds and S_0 keto become closer, which could facilitate the ESIntraPT. The NCCC dihedral angles of all HBO and its derivatives both in S_0 and S_1 states are almost 0° indicating that all structures are planar. Even adding the substituents, the dihedral angles do not change and the planarity of all compounds is kept both in enol and keto forms.

Thus, these substituents can influence the hydrogen bonding capability by making O–H bond stronger compared to HBO but do not affect the NCCC angle of its structural skeleton.

3.3.3 UV-Vis Absorption and Fluorescence Spectra

Quantum calculations are a useful tool to reproduce the experimental spectra and to predict unreported spectra with reliable methods. The intensities are computed using time-dependent DFT in Gaussian 09. Frank-Condon absorption and emission are performed from the equilibrium structures of ground (S_0) and excited states (S_1), respectively. The highest peak (π-π*) corresponds to 0-0 transition as well as its second highest one (n-π*). Photophysical properties of *m*-MeHBO, MHBO, CNHBO, HBOMe, HBOM, HBOF, HBOCl, HBOA, HBOE, and *m*-MeHBON at TD-B3LYP/6-311+G* level in the gas phase are summarized in Table 3.3 (calculated enol absorption and keto emission). The main transition of UV-vis absorption is π-π* (or HOMO→LUMO).

3.3.3.1 Absorption Spectra

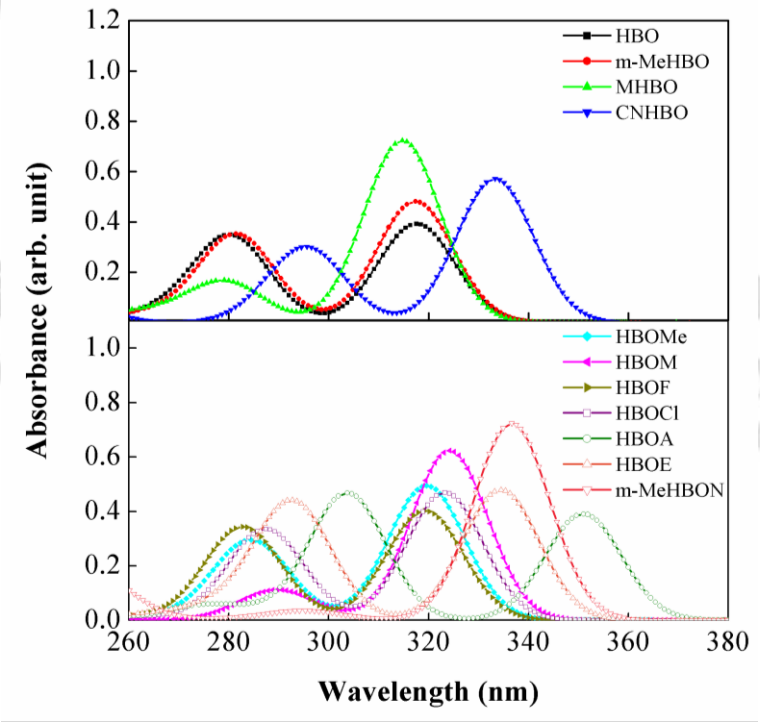

Figure 3.2. Calculated absorption spectra of HBO and its derivatives performed at TD-B3LYP/6-311+G* level in the gas phase.

Table 3.3 Electronic and photophysical properties of HBO and its derivatives computed at TD-B3LYP/6-311+G* level in the gas phase. Calculated enol absorption and keto emission (nm, eV), oscillator strength (*f*), and major contributions (%).

	Absorption								**Emission**			
	Calculation							**Experiment (nm)**	**Calculation $S_1 \rightarrow S_0$**			**Experiment (nm)**
	π-π*				**n-π***							
	nm	**eV**	***f***	**MOs (% contribution)**	**nm**	**eV**	***f***	**π-π***	**nm**	**eV**	***f***	
HBO	318	3.90	0.393	HOMO→LUMO (92%)	280	4.42	0.346	335 [a] [91]	476	2.61	0.189	466 [a] [91]
***m*-MeHBO**	317	3.91	0.478	HOMO→LUMO (92%)	281	4.40	0.358	334 [d] [126]	473	2.62	0.185	485 [d] [126]
MHBO	314	3.94	0.723	HOMO→LUMO (94%)	279	4.44	0.171	336 [c] [69]	458	2.71	0.163	466 [c] [69]
CNHBO	333	3.72	0.572	HOMO→LUMO (93%)	296	4.19	0.295	353 [b] [102]	467	2.66	0.227	497 [b] [102]
HBOMe	320	3.88	0.495	HOMO→LUMO (92%)	284	4.36	0.295	-	475	2.61	0.208	-
HBOM	324	3.82	0.623	HOMO→LUMO (95%)	290	4.28	0.112	-	466	2.66	0.227	-

HBOF	319	3.88	0.403	HOMO→LUMO (91%)	283	4.38	0.344	-	482	2.57	0.181	-
HBOCl	323	3.84	0.469	HOMO→LUMO (92%)	287	4.31	0.335	-	487	2.55	0.197	-
HBOA	351	3.53	0.391	HOMO→LUMO (95%)	304	4.08	0.468	351 [e] [69]	644	1.93	0.117	510 [e] [69]
HBOE	335	3.71	0.479	HOMO→LUMO (95%)	293	4.24	0.437	345 [e] [69]	563	2.20	0.153	480 [e] [69]
***m*-MeHBON**	337	3.68	0.724	HOMO→LUMO (97%)	295	4.20	0.035	-	483	2.57	0.201	-

In [a] an argon matrix, [b] solid state, [c] cyclohexane, [d] 3-methylpentane, and [e] chloroform.

From calculated absorption (Figure 3.2), there are two absorption peaks for *syn*-enol form of HBO and its derivatives which are attributed to π-π* (longer wavelength) and n-π* (shorter wavelength) transitions. Calculated absorption maxima of HBO are 318 nm (π-π*) and 280 nm (n-π*) nm with oscillator strength (*f*) of 0.393 and 0.346, respectively. These values are in good agreement with the experiment data both in gas phase [91] and non-polar solvent [97]. For 4′-position substitution such as *m*-MeHBO, MHBO and CNHBO, the spectral position of enol absorption of *m*-MeHBO shows similar characteristic peaks to that of HBO in which two peaks are computed to be at 317 nm and 281 nm with *f* of 0.478 and 0.358, respectively. This slightly higher *f* compared to those of HBO could be from the weaker electron donating capability of methyl group. In addition, MHBO having a methoxy group as electron donor shows absorption peak at 314 and 279 nm with very high *f* of 0.723 (π-π*) and 0.171 (n-π*). Similarly, strong electron withdrawing (-CN) group of CNHBO shows absorption maxima at 333 nm and 296 nm with *f* values of 0.572 and 0.295, respectively. A large redshifted absorption compared to HBO, observed in CNHBO corresponding to lower energy gap than that of HBO, agrees well with experiments [102]. The slight blueshifted absorption spectra of *m*-MeHBO and MHBO compared to HBO for π-π* (n-π*) are computed to be at 317 (281) and 314 (279) nm, respectively. This slight blueshifted absorption of these compounds might be caused by electron donating ability of O atom which is lower than that of C atom resulting in larger vertical excitation energy. For 6-position substitution, the absorption spectra of all HBO derivatives show redshifted corresponding to lower vertical excitation energies than that of HBO. Electron donors (HBOMe, HBOM, HBOF, and HBOCl) show slightly redshifted with peaks in range of 319-324 nm while HBOA and HBOE show large redshifted with peaks at 351 and 335 nm for π-π* transitions. In addition, electron donor substituted on 4′-position and electron acceptor substituted on 6-position of *m*-MeHBON also give redshifted absorption with peak at 337 nm (*f* = 0.724) for π-π* and n-π* transition (very small *f*). This red shift may be caused by push-pull dipolar property.

3.3.3.2 Emission Spectra

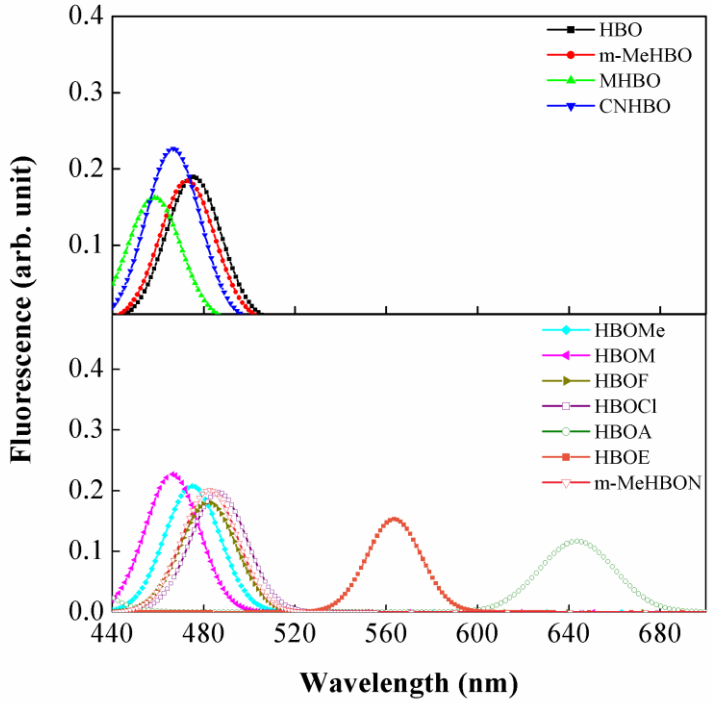

Figure 3.3. Calculated fluorescence spectra of HBO and its derivatives computed at TD-B3LYP/6-311+G* in the gas phase.

Fluorescence emission (Figure 3.3) of keto HBO and its derivatives computed at B3LYP/6-311+G* in the gas phase shows different wavelength as summarized in Table 3.3. The computed keto emission of HBO at 476 nm agrees with gas phase experiment [91]. For HBO derivatives substituted on 4′-position of phenol fragment, maxima emission spectra of *m*-MeHBO, MHBO, and CNHBO are 473, 458, and 467 nm, respectively, which are blueshift relative to HBO (Table 3.3). These blue shifts especially the electron acceptor mesomeric effects may be taken into account by large π-electron density at the 4′-position. While, the electron donor shows little contribution of mesomeric effect leading to π-electron density disappearance. Our computed results of *m*-MeHBO, MHBO, and CNHBO are in good agreement with experiment data [69, 102, 128]. For 6-position substitution, electron donors (HBOMe and HBOM) show blueshifted emission with maxima at 475 and 466 nm while electron acceptors (HBOF, HBOCl, HBOA, and HBOE) show redshifted emission with maxima at 482, 487, 644, and 563 nm, respectively. The red shift is also found for *m*-MeHBON

emission spectrum because of NO_2 acting as strong withdrawing group on 6-position of benzoxazole. These red shifts might be from a large π-electron density contributed by π-conjugation at carbon 6 in benzoxazole ring.

From all computed emission results, the effect of substitutions of electron donating (*m*-MeHBO and MHBO) and withdrawing (CNHBO) groups on the phenol fragment and electron donating (HBOMe and HBOM) on benzoxazole fragment makes the position of keto emission peak shift to shorter wavelength (blueshift) in the gas phase, while withdrawing (HBOF, HBOCl, HBOA and HBOE) groups give redshifted emission compared to the parent compound (HBO). In addition, both electron donating on 4′-position and electron withdrawing substituents on 6-position (*m*-MeHBON) give redshifted emission.

3.3.4 Energy Diagram of HOMO and LUMO Levels and Frontier Molecular Orbitals

Figure 3.4 shows calculated HOMO and LUMO energy levels of enol absorption (top) and keto emission (bottom), respectively. The energy levels of HOMO and LUMO, and HOMO-LUMO gap depend on substitution of the parent compound (HBO).

For enol absorption, energy differences between HOMO of HBO and HBO derivatives as well as LUMO are compared. HOMO and LUMO energy levels of HBO with electron donor (*m*-MeHBO, MHBO, HBOMe, HBOM, and *m*-MeHBON) are higher than that of HBO while, HBO with electron acceptor substituents (CNHBO, HBOF, HBOCl, HBOA, and HBOE) are lower compared to HBO. These indicate that mesomeric effect plays important role in the variations of energy level. The HOMO energy levels of HBO having methyl group in *m*-MeHBO (4.34 eV) and HBOMe (4.30 eV) are very similar to that of HBO, while methoxy group in MHBO (4.31 eV) and HBOM (4.19 eV) slightly raised HOMO energy level as well as *m*-MeHBON (4.01 eV). The LUMO energy level of HBO having electron withdrawing groups such as CNHBO, HBOF, HBOCl, HBOA and HBOE is stabilized to be lower than its HBO especially CNHBO at 4′-positon and HBOA at 6-position. An electron-donating group raises

the HOMO energy level of the compounds more than its LUMO energy level while an electron-withdrawing group stabilizes LUMO energy level more than HOMO energy level. Overall, HOMO-LUMO gaps of all derivatives are lower than that of HBO (4.35 eV) resulting in red shift enol absorption.

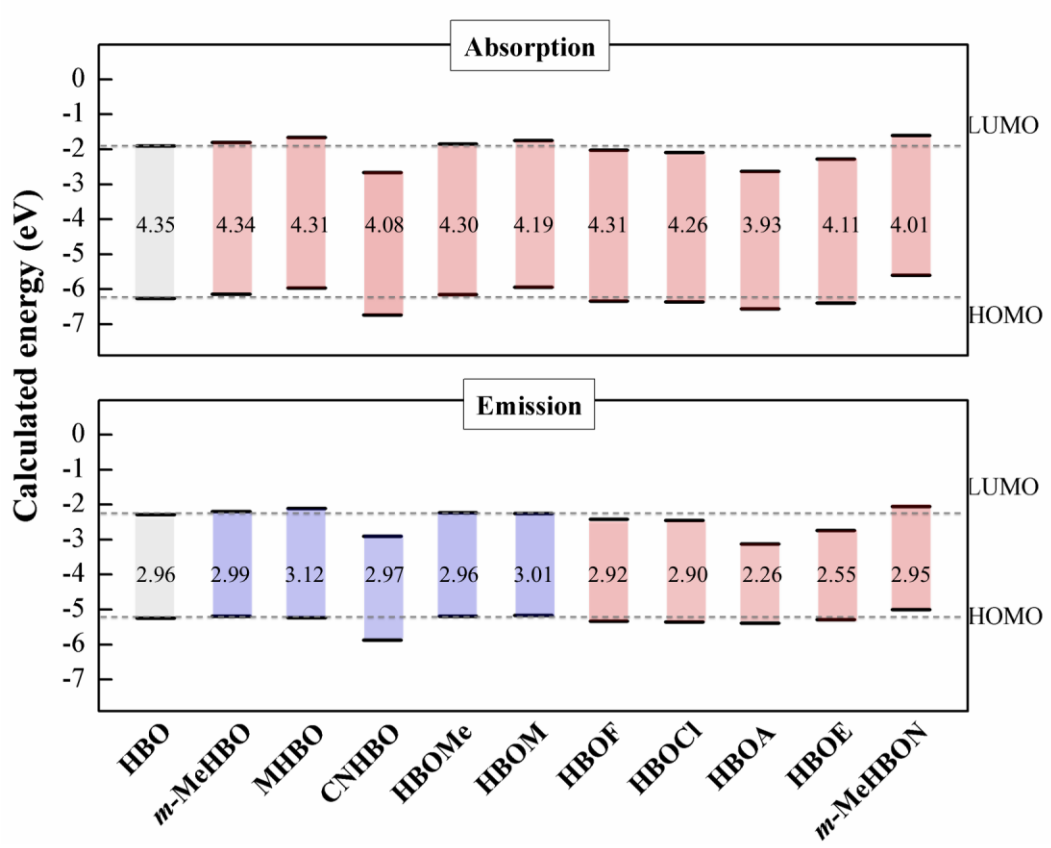

Figure 3.4. Diagram of calculated HOMO and LUMO energy levels as well as HOMO-LUMO gaps (eV) at TD-B3LYP/6-311+G* level of enol absorption and keto emission of HBO and its derivatives.

For keto emission, the effect of substituents to keto tautomers gives the same trend as in the enol in which the electron-donating group raises the HOMO energy level but the electron-withdrawing group lowers LUMO energy level compared to HBO. The energy gap of HBO is 2.96 eV. Adding electron donors especially in 4′-position such as *m*-MeHBO (2.99 eV) and MHBO (3.12 eV) and at 6-positon such as HBOMe (2.96 eV) and HBOM (3.01 eV) as well as electron acceptor (CNHBO), the blueshift emission is found when compared to HBO. An electron-donating group raises the HOMO energy level of the compounds more

than its LUMO energy level, while; CN in CNHBO stabilizes both HOMO and LUMO energy level. Moreover, energy gaps of electron acceptors at 6-position such as HBOF, HBOCl, HBOA, and HBOE are 2.92, 2.90, 2.26 and 2.55 eV, respectively exhibiting redshifed emission as displayed in Table 3.3 as well as two groups substitution in *m*-MeHBON (2.95 eV). Electron-withdrawing group stabilizes LUMO energy level well especially in HBOA and HBOE in according with a positive effect on the ESIntraPT fluorescence.

The frontier molecular orbitals describing electron densities of enol and keto HBO and its derivatives are analyzed to investigate the nature of electronic transition upon photoexcitation and displayed in Figure 3.5. Note that the HOMO and LUMO are assigned to π and π* character, respectively. It is well known that the proton transfer in the excited state takes place on this π-π* state [140]. The main contributions of electronic transition of HBO and its derivatives are HOMO (π) to LUMO (π*) as summarized in Table 3.3 for the gas phase. The electron density contributions of HBO and its derivatives both in the gas phase and solution are in the range of 91% - 97% (HOMO→LUMO). The distribution is delocalized over the whole molecules of enol and keto forms for HBO and its derivatives. For substituents on 4′-position of phenol fragment, π-electron density (HOMO) of keto is considerably lower than that of its enol (Figure 3). Because of the disappearance of π-electron at 4′-position of phenol, it suggests that negative inductive effect is involved rather than mesomeric effect [69], resulting in a low contribution of electrons at 4′-position of phenol leading to blue shift emission of keto.

Both electron-donating and electron-withdrawing groups substituted at 4′-position of HBO cause emission blueshifted. However, at 6-positon substitutions, the electron-donating group gives blueshifted emission while electron withdrawing gives redshifted emission compared to HBO. The redshifted emission can be observed due to higher electron withdrawing capability at 6-position. The compounds that can give the keto emission are HBOM, HBOMe, HBO, HBOF, HBOCl, HBOE, and HBOA ranging from blue to red shift,

respectively, which is in the order of increasing the electron-withdrawing ability of substituents.

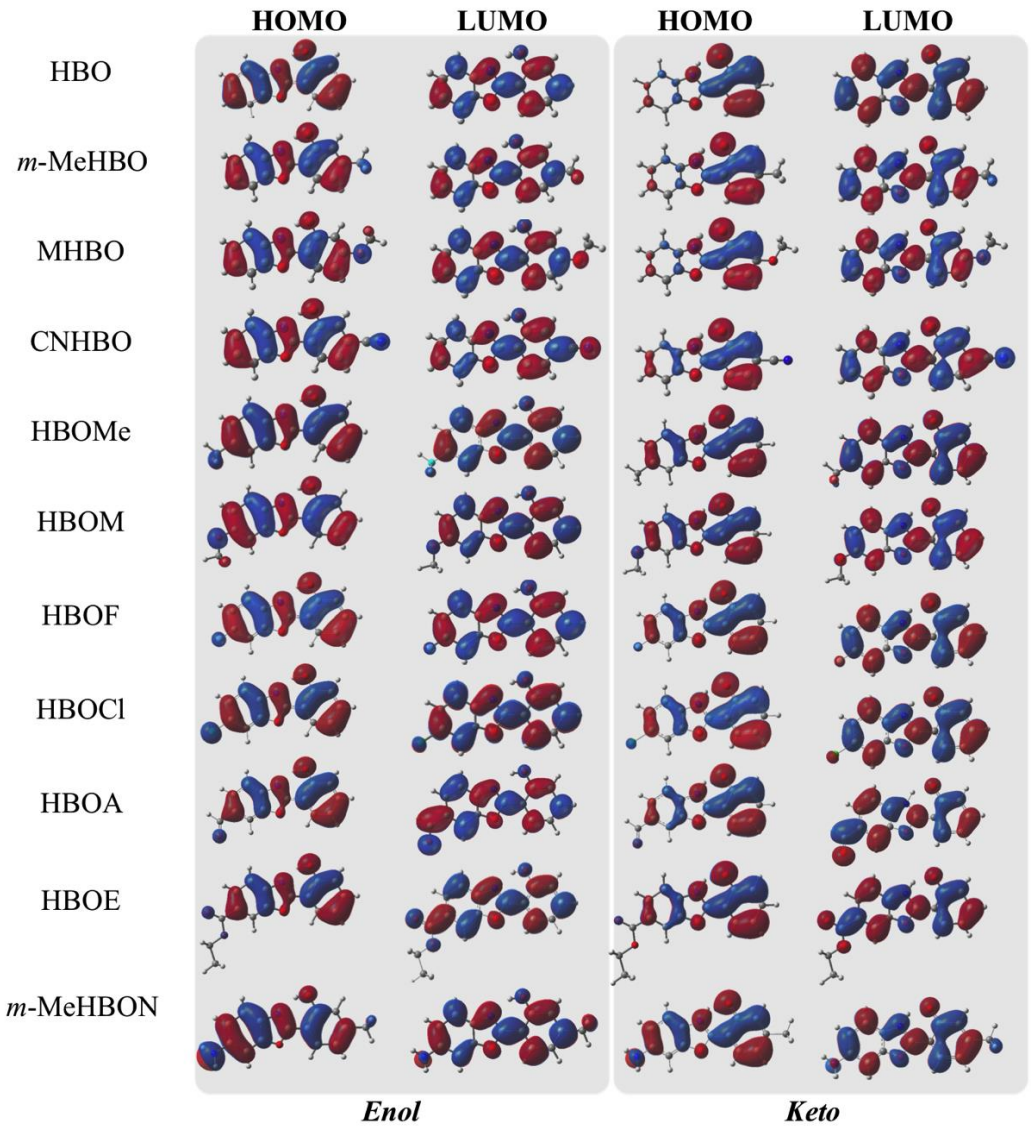

Figure 3.5. Frontier molecular orbitals of enol and keto for HBO and its derivatives computed at TD-B3LYP/6-311+G* in the gas phase.

3.4 Chapter Summary

The effect of electron donating and withdrawing substituents on the absorption and fluorescence spectra of the 4′-position of phenyl moiety and 6-position of benzoxazole of HBO was systematically investigated using five different DFT functionals. The popular B3LYP exchange-correlation functional is found to provide the best results in predicting the absorption spectrum close to experimental data. In ground state optimization, enol forms of HBO and its derivatives are found to be more stable than those of keto forms, while it is opposite in first-lowest excited state.

Simulated absorption and emission spectra of HBO and its derivatives from TD-B3LYP calculation are in agreement with the experimental data. The effect of electron donating groups in *m*-MeHBO and MHBO gives blueshifted while electron withdrawing group in CNHBO shows redshifted absorption. Overall, the effect of electron donor raises the HOMO energy level of the compounds more than its LUMO energy level while electron acceptor stabilizes LUMO energy level more than HOMO level. For keto emission, HBO having electron donating groups (*m*-MeHBO and MHBO) and withdrawing group (CNHBO) at 4′-position on the phenol fragment as well as electron donating groups (HBOMe and HBOM) at 6-position on the benzoxazole fragment make the position of keto emission peak shift to shorter wavelength (blueshift). However, HBO derivatives having electron-withdrawing groups (HBOF, HBOCl, HBOA and HBOE) give redshifted emission compared to the parent compound (HBO).